Journal of Industrial Microbiology & Biotechnology (1997) 18, 204–212
© 1997 Society for Industrial Microbiology 1367-5435/97/$12.00

Effects of nutrient dosing on subsurface methanotrophic populations and trichloroethylene degradation

SM Pfiffner[1], AV Palumbo[1], TJ Phelps[1] and TC Hazen[2]

[1]*Environmental Sciences Division, Oak Ridge National Laboratory, PO Box 2008, Oak Ridge, TN 37831-6036;*
[2]*Westinghouse Savannah River Technology Center, Aiken, SC, USA*

In *in situ* bioremediation demonstration at the Savannah River Site in Aiken, South Carolina, trichloroethylene-degrading microorganisms were stimulated by delivering nutrients to the TCE-contaminated subsurface via horizontal injection wells. Microbial and chemical monitoring of groundwater from 12 vertical wells was used to examine the effects of methane and nutrient (nitrogen and phosphorus) dosing on the methanotrophic populations and on the potential of the subsurface microbial communities to degrade TCE. Densities of methanotrophs increased 3–5 orders of magnitude during the methane- and nutrient-injection phases; this increase coincided with the higher methane levels observed in the monitoring wells. TCE degradation capacity, although not directly tied to methane concentration, responded to the methane injection, and responded more dramatically to the multiple-nutrient injection. These results support the crucial role of methane, nitrogen, and phosphorus as amended nutrients in TCE bioremediation. The enhancing effects of nutrient dosing on microbial abundance and degradative potentials, coupled with increased chloride concentrations, provided multiple lines of evidence substantiating the effectiveness of this integrated *in situ* bioremediation process.

Keywords: *in situ* bioremediation; subsurface; methanotrophs; TCE; nutrient availability

Introduction

In situ bioremediation field studies involving chlorinated solvents [13,31,32] have demonstrated that biostimulation of indigenous methane-oxidizing bacteria by the addition of methane can enhance cometabolic biodegradation of trichloroethylene (TCE). TCE is a subject of *in situ* bioremediation efforts because it is one of the most common groundwater contaminants in the United States and is related to health concerns [6,20,30,36]. Thus, the mechanisms for remediating TCE-contaminated subsurface environments have been the subject of considerable research and development. Aerobic biodegradation of TCE has been demonstrated in both pure and mixed microbial cultures [1,9–11,18,21,33,35,37,39].

Nutrient availability is likely to be critical for microbial growth and contaminant biodegradation during *in situ* bioremediation. Previous investigators [15,24,25,29] have demonstrated enhanced microbial growth, acetate incorporation, and TCE mineralization when sediments were supplemented either with nutrients alone (phosphorus and nitrogen) or in combination with the addition of electron acceptors and donors. Understanding nutrient dispersion and bioavailability in the subsurface may be important in controlling contaminant degradation and, thus, in the effectiveness of *in situ* bioremediation processes.

This article examines changes in methanotrophic populations and aerobic TCE-degradative capacities in groundwater, as part of the US Department of Energy (DOE) Office of Technology Development Integrated Demonstration for the *in situ* bioremediation of chlorinated solvents at the Savannah River Site (SRS) [12]. The analyses focus on groundwater sampling locations with respect to the location of the horizontal injection and extraction wells. Spatial and temporal relationships of degradative populations and activities were investigated to examine the effects of methane and nutrient dosing.

Correspondence: AV Palumbo, Environmental Sciences Division, Oak Ridge National Laboratory, PO Box 2008, Oak Ridge, TN 37831-6036, USA
Received 13 November 1995; accepted 12 September 1996

Materials and methods

Study site

The study site (Figure 1) on the SRS reservation in Aiken, South Carolina, included a 7000 m^2 area contaminated mainly with TCE. The water table was 36 m below ground surface (bgs), and the primary location of the TCE contamination was 27–45 m bgs. The geological, geochemical, hydrological, and microbiological properties of the demonstration site [7] were characterized before the initiation of the *in situ* bioremediation campaigns.

Two horizontal wells skewed to each other at an approximately 27° angle, with the upper extraction well positioned in the vadose zone at a depth of 24 m and the lower injection well at 53 m, constituted the delivery system. The angle and position of the extraction and injection horizontal wells allowed methane to travel to the extraction well from both sides (Figure 1). Gaseous nutrients were delivered to the subsurface at a rate of 5.67 m^3 min^{-1} by injection into the lower horizontal well (AMH-1). The extraction of air and contaminants was accomplished by vacuum extraction through the upper horizontal well (AMH-2) at 6.80 m^3 min^{-1}. *In situ* air stripping (air sparging plus soil vapor extraction, US Patent 4 832 122 [5]) was used at the site before methane injection [19]. Extensive groundwater

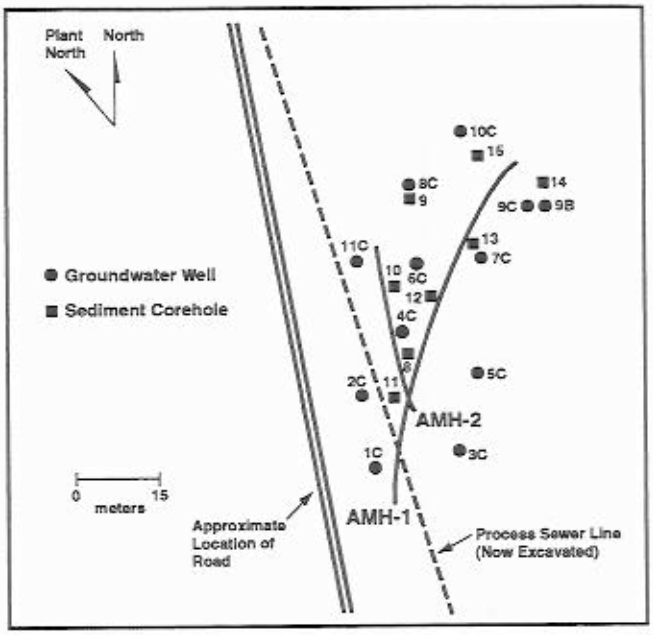

Phase:	Description:
4% Methane	Continuous injection of 4% methane in air, with vacuum extraction
Pulsed Methane	Pulsed injection of 4% methane in air and air only, with vacuum extraction
Multiple Nutrient	Pulsed injection of methane and air with continuous injection of 0.07% nitrous oxide and 0.007% triethyl phosphate, with vacuum extraction
Post-test	no injection or vacuum extraction

Figure 1 Plan view of the location of 12 groundwater-monitoring wells (●) and eight sediment coreholes (■) with respect to the position of the injection horizontal well (AMH1), extraction horizontal well (AMH2), and sewer line (—). Notice the angle and positions of the (24-m depth) extraction horizontal well (AMH2) and lower (53-m depth) injection horizontal well (AMH1). The water table was located at a depth of 36 m. The primary TCE contamination was between the depths of 27–45 m. The table describes the treatment phases.

sampling (wells 1C–11C and 9B, Figure 1) and sediment sampling (coreholes 8–15, Figure 1) were implemented to monitor the effects of the nutrients that were added through the injection horizontal well.

Bioremediation campaigns

A series of increasingly aggressive approaches for biostimulation of indigenous TCE-degrading populations were implemented over a 17-month period. A control phase (phase 1) without treatment was followed by vacuum extraction (phase 2), air injection (phase 3), injection of 1% methane in air (phase 4, US Patent 5 326 703) [14], injection of 4% methane in air (phase 5), pulsed methane and air injection (phase 6), continuous addition of triethyl phosphate (0.007%) (US Patent 5 480 549 [3]) and nitrous oxide (0.07%) in air with pulsed additions of methane and air (phase 7), and a final post-test phase without treatment (phase 8) [13].

Phases 1–4 were conducted from January 1992 to August 1992 and reported in previous publications [13,25,26]. This work focuses on phases 5–8, which were conducted from August 1992 to May 1993. Phases 5–8 were examined to determine the effects of nutrient dosing; these phases were chosen based on the available data for methane concentration in groundwater, which started with the 4% methane injection. Therefore, important background information prior to the 4% methane injection is provided. The 1% methane injection significantly increased the average density of methanotrophs from <1 cell ml^{-1} during phases 1–3 to 2400 cells ml^{-1} during 1% methane injection (phase 4) [13,25,26]. TCE mineralization potential, as measured by the degradation of radiolabeled TCE to CO_2 (under enriched conditions), increased from an average and standard error of 3.4 ± 0.4 for phases 1–3 to 9.8 ± 1.31 for phase 4 [25,26]. In addition, the nutrient-limiting conditions in the subsurface have been demonstrated at this site [25,29].

Groundwater analyses

Groundwater was sampled twice monthly from the vertical monitoring wells according to documented SRS sampling protocols [12]. Monitoring wells were pumped until conductivity and pH were stabilized (after $\geq$3 pore volumes) and then 10 L of groundwater collected in sterile polypropylene containers. Studies of microbial activity and enumeration in the groundwater samples were conducted at the SRS laboratory. Retrieved groundwater samples were stored at 4°C until they were processed in the laboratory (within 2–4 h from the recovery from the monitoring well). Physical and chemical analyses were performed on-site or subcontracted by SRS to laboratories certified by the US Environmental Protection Agency [12].

Monitoring well locations

The orientation of the horizontal wells and extensive collection of data from the demonstration allowed determination of a zone effect, a region where microbial and chemical responses were more immediate and more noticeable. On the basis of the site design and the data, groundwater-monitoring wells MHT-2C, 4C, 6C, 7C, and 11C were considered to be within the zone of effect from both the injection and extraction horizontal wells (Figure 1). Groundwater-monitoring wells MHT-1C, 3C, 5C, 8C, 9C, 10C, and 9B which likely experienced less or delayed effects from the treatment phases, were considered to be in an area adjacent (outlying) to the zone of effect (Figure 1).

Sediment sampling and corehole location

Before multiple-nutrient injection ceased, sediments were sampled by a split-spoon coring technique according to documented SRS sampling protocols [12]. Eight coreholes (MHC-8 to MHC-15) were located throughout the demonstration site (Figure 1).

Microbial enumeration

Methane-oxidizing populations were assessed by the turbidimetric three-tube most-probable-number (MPN) technique [26]. For MPN analysis, groundwater was inoculated into a medium which contained phosphate-buffered mineral salts, adjusted to pH 7.1, and supplemented with an amount of methane (vol:vol) equal to 5% of the headspace [26].

The test tubes were incubated for 30 days at 25°C. Microbial growth was visually assessed at 14 and 30 days.

TCE mineralization

Time course enrichments were used to estimate the mineralization of radiolabeled TCE to radiolabeled CO_2. The experiments used 10 ml of groundwater, 0.5 μCi of carrier-free [1,2-^{14}C]-TCE (Sigma Chemical Co, St Louis, MO, USA), and 2 ml of double-strength methanotrophic medium (except for phosphate, which was added for a final concentration of 0.33 mM) [26]. As nutrient supplements, yeast extract and trypticase were each added to produce a final concentration of 20 μg L^{-1} [25–27]. Methane and propane, as additional supplements, were added in amounts equal to 3% and 5% (vol:vol) of the headspace, respectively. The test tubes were incubated for 30 days at room temperature, inhibited with 0.4 ml of 2 M NaOH, and frozen until analyzed. The test tubes were acidified with 0.5 ml of 6 M HCl 1 h before radioactive CO_2 levels were determined by gas chromatography-gas proportional counting. A Shimadzu 8A gas chromatograph equipped with a thermal conductivity detector (HNU Systems, Newton, MA, USA) and a Packard 894 gas proportional counter were used to determine the headspace $^{14}CO_2$ [22,27].

Chemical analyses

Methane concentration in groundwater samples was measured on a Hewlett-Packard 5890A gas chromatograph equipped with either a thermal conductivity or flame ionization detector and compared to standards of methane-saturated deionized H_2O [8]. The detection limit for methane was ≤0.1% in groundwater samples. Conductivity was measured using a Hydrolab Surveyor model (Hydrolab Inc, Houston, TX, USA) as described in the test plan [12]. Chloride was analyzed by argentometric titration on sediment samples, which were stored at 4°C [2].

Statistical analyses

For statistical analyses, log transformations were performed for three parameters: (1) cell concentration (cells ml^{-1}+1) for methane-oxidizers (avoiding the log of zero); (2) methane concentration (μg L^{-1}); and (3) the percentage of radiolabeled TCE mineralized. Einsight pattern recognition software (Infometrix Inc, Seattle, WA, USA) was used for hierarchical cluster and principal component analyses. Hierarchical cluster analysis (HCA) related samples to each other on a similarity index (SI) scale, on which 0 represented no similarity between samples and 1 represented identical samples. We used the Euclidean distance metric and the incremental clustering technique for the HCA analysis. This analysis was conducted for each assay on data from 4% methane injection through post-test phases.

Principal component analysis (PCA) was used to determine the factors in the dataset that accounted for the most variance. Those factors carried more weight (more sample variance) in defining the variance among sample clusters. Linear regressions were calculated with Lotus 1.2.3, release 4.0 (Lotus Development Corp, Cambridge, MA, USA).

Contour maps were produced by interpolation of the data (methane concentration, methanotrophic density, percentage of TCE mineralized, and chloride concentration) averaged for each groundwater-monitoring well or corehole over the multiple-nutrient injection phase. The software program utilized was Sigmaplot, version 2.10 (Jandel Corporation, San Rafael, CA, USA).

Results

Methane concentration in groundwater

The monitoring wells were clustered into three methane dosing groups (groups G-1, G-2, G-3; see Table 1) on the basis of the HCA conducted on methane concentrations measured in groundwater recovered from the monitoring wells during phases 5–8. Monitoring wells within group G-1 clustered at a similarity index (SI) of 0.85. The SI is an indicator of the degree to which the patterns were similar among wells from a scale of 0–1. This well group related to well group G-2, which had an SI of 0.51. Wells in group G-3 showed no similarity (SI = 0) to either G-1 or G-2. Monitoring wells in group G-1 were located outside and beyond the horizontal wells and were adjacent to the zone of effect (Table 1 and Figure 1). Wells in group G-2 were positioned between both horizontal wells or near the injection horizontal well. Group G-3 wells were located near the extraction horizontal well (Table 1 and Figure 1). All monitoring wells from both groups G-2 and G-3 were considered to be within the zone of effect.

A plot of the average groundwater methane concentration (log μg L^{-1}) for each of the three well groups over the 4% methane-injection phase through the post-test phase (Figure 2) demonstrated that wells within the zone of effect (groups G-2 and G-3) were exposed to higher concentrations of methane (≥100 μg L^{-1}) in the groundwater than were the remote wells (group G-1). In the remote wells, methane concentrations were less than 100 μg L^{-1} (Figure 2). PCA indicated that the first four sampling periods (days 174, 188, 202, and 214) during the 4% methane-injection phase and day 391 (during the multiple-nutrient injection phase) accounted for the most variance among the well groups. Those days showed the largest observed sample differences in methane concentration.

Effect of methane dosing on methanotrophs

Prior to methane injection, methane was not detected in groundwater. Before 1% methane injection, methanotrophic densities averaged <1 cell ml^{-1}. Within 22 days of 1% methane injection, the average methanotrophic density in groundwater increased to 1.5 cells ml^{-1} (data not shown). After day 36 of 1% methane injection, all groundwater-monitoring wells exhibited increases in methanotrophs with an average density of 15 cells ml^{-1}. This rapid increase in methanotrophs was the first impact of methane dosing. By the end of 1% methane injection (day 160), the average methanotrophic density had increased to 2400 cells ml^{-1} (data not shown).

To understand the effects of methane concentration on methanotrophic growth, methanotrophic densities (Figure 3) in groundwater-monitoring wells were compared to each other using the same G-well grouping determined by the HCA on groundwater methane concentration (Table 1). Averaged methanotrophic densities for each group were plotted from the beginning of the 4% methane-

Table 1 Sampling wells clustered by methane gas concentration (G groups), methanotrophic bacterial density (B groups), and TCE degradation (T groups). Hierarchical cluster analysis on the methane concentration, methanotrophic density, and TCE mineralization results from phases 5–8 was performed using the Euclidean distance metric and incremental clustering technique

Clustered by	Groups			
Methane (G)	**G1**		**G-2**	**G-3**
	1C, 3C, 5C, 8C, 9C, 10C, 9B		4C, 6C, 7C	2C, 11C
Methanotrophs (B)	**B-1**	**B-2**	**B-3**	
	8C, 9B	1C, 3C, 5C, 9C, 10C	2C, 4C, 6C, 7C, 11C	
TCE Degradation (T)	**T-1**	**T-2**	**T-3**	**T-4**
	2C, 5C, 6C, 9C, 11C	1C, 3C	7C, 8C, 10C, 9B	4C

injection phase through the post-test phase (Figure 3). Group G-1 (adjacent to the zone of effect) experienced lower methane concentrations (≅100 μg L^{-1}) (Figure 2) and exhibited methanotrophic densities ranging from 10^1 to 10^3 cells ml^{-1} (Figure 3). In contrast to group G-1, groups G-2 and G-3 which were exposed to higher methane concentrations (≅500 μg L^{-1}) (Figure 2) during the 4% methane injection, showed methanotrophic densities ranging from 10^3 to 10^5 cells ml^{-1} (Figure 3). Increases in methanotrophic densities coincided with the elevated methane dosing concentration (Figures 2 and 3).

When densities of methanotrophs were examined for changes over the treatment phases, trends were identified with respect to monitoring well groups (Figure 3). During the 4% methane injection phase, groups G-1 and G-3 showed increased densities of methanotrophs; these increases were supported by the positive linear regression slopes, 0.011 and 0.004, respectively. At the same time, group G-2 showed a negative slope (–0.010) which was indicative of a decrease in abundance of methanotrophs. Despite the negative slope, group G-2 nevertheless had high densities of methanotrophs. With the pulsed injection phase, all groups showed increased abundance of methanotrophs and positive slopes (0.003, 0.005, and 0.0052 for

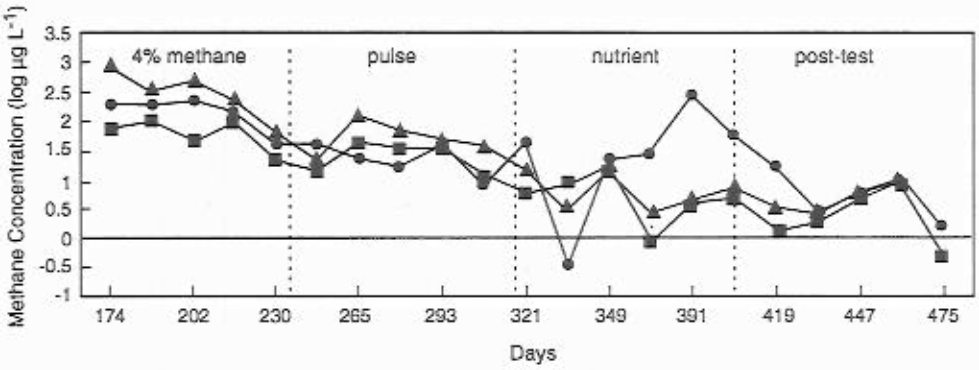

Figure 2 Average methane concentration (log μg L^{-1}) in groundwater from the monitoring wells, which were grouped on the basis of hierarchical cluster analysis. The depicted days (174 to 489) include the 4% methane-injection phase through the post-test phase. Monitoring wells were clustered according to three methane dosing groups: wells MHT-1C, 3C, 5C, 8C, 9C, 10C, and 9B (group G-1, ■); wells MHT-4C, 6C, and 7C (group G-2, ●); wells MHT-2C and 11C (group G-3, ▲). Groups G-3 (near the extraction horizontal well) and G-2 (between both horizontal wells) were considered to be within the zone of effect, whereas group G-1 was adjacent to the zone of effect.

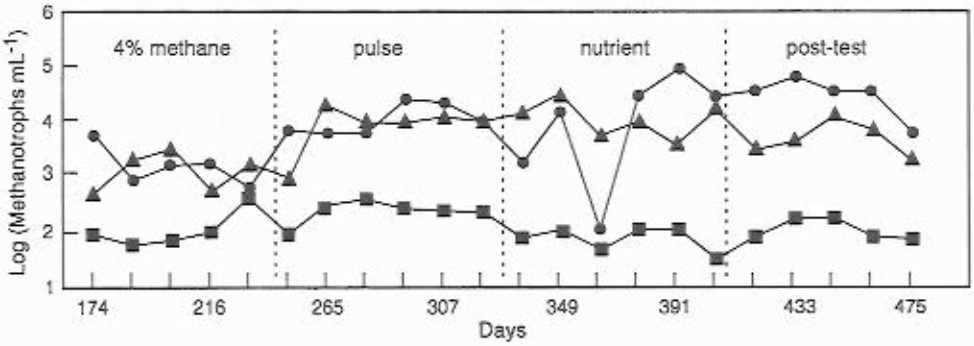

Figure 3 Densities of methanotrophs in groundwater (log cells ml^{-1}) averaged for specific groups of monitoring wells during the 4% methane injection through the post-test phase. The monitoring wells were grouped on the basis of the methane concentration hierarchical cluster analysis (group G-1, ■; group G-2, ●; group G-3, ▲). Groups G-3 (near the extraction horizontal well) and G-2 (between both horizontal wells) were considerd to be within the zone of effect, whereas group G-1 was adjacent to the zone of effect.

groups G-1, G-2, and G-3, respectively). With respect to the multiple-nutrient injection phase, groups G-1 and G-3 displayed negative slopes (–0.001 and –0.004, respectively), which supported the slight decrease observed in densities of methanotrophs in groundwater from those wells. Increases in densities of methanotrophs following multiple-nutrient injection were indicated by the 0.022 slope observed for groundwater from the G-2 monitoring wells. After injection and extraction operations ceased, all groups exhibited negative slopes and decreasing densities of methanotrophs following a lag period (Figure 3).

Hierarchical clustering based on methanotrophic densities

To provide further insight on the spatial and temporal effect of methane dosing, HCA was performed on the groundwater densities of methanotrophs. The analysis revealed three different groups of groundwater-monitoring wells (groups B-1, B-2, B-3) that did not fully correspond to the methane dosing groups (groups G-1 to G-3) (Table 1). The wells in groups B-1 and B-2 were located adjacent to the zone of effect and were closely related to each other (SI of 0.55). Group B-3 wells were located within the zone of effect and were unrelated to those in groups B-1 and B-2. Group B-1 (Table 1) displayed the lowest densities of methanotrophs (10–100 cells ml^{-1}). In contrast, densities of 100–1000 cells ml^{-1} were observed in group B-2 (see Table 1). Groups B-1 and B-2 together consisted of the monitoring wells found in group G-1 (outside the more affected zone), which had low methane dosing (Table 1). The highest abundance of methanotrophs (>1000 cells ml^{-1}) was found in group B-3. Group B-3 contained the groundwater-monitoring wells found in both groups G-2 and G-3, which had higher methane dosing and was within the zone of effect (Table 1). Because <1 methanotroph ml^{-1} was observed throughout the demonstration site prior to methane injection, the HCA of densities of methanotrophs after injection further substantiated the trend that groundwater in which higher levels of methane were measured exhibited higher abundances of methanotrophs.

Effect of methane on TCE mineralization

Results of the TCE-degradation potential experiments from the beginning of the 4% methane-injection phase through the post-test phase (Figure 4) were compared by using the same methane dosing groups (G-1, G-2, and G-3) determined by HCA on methane concentration (Table 1). TCE mineralization was not observed in uninoculated controls. The methane dosing groups showed similar mineralization potential during the 4% methane- and the pulsed-methane injection phases (Figure 4). With the injection of multiple nutrients, the G-2 group of wells, which consisted of wells within the zone of effect, showed rapid increase in TCE-degradation capacity (Figure 4). Monitoring wells in group G-3, also within the zone of effect but located near the extraction horizontal well, showed a slight increase in TCE-mineralization potential during the early part of the multiple-nutrient injection phase (Figure 4). Monitoring wells located adjacent to the zone of effect (group G-1) exhibited a dramatic, although delayed, increase in TCE degradation potential (Figure 4). During the pulse injection phase, TCE degradation potential in group G-1 increased but the delay likely resulted from slow and diminished migration of nutrients to the remote wells similar to the diminished methane concentration (Figure 2). However, the methane arriving at group G-1 wells was utilized within 20–50 days as indicated by the maximal methane level followed by decreasing methane concentrations and by increased densities of methanotrophs (Figure 2). Similarly, within 20–50 days after the onset of multiple-nutrient injection, the TCE degradation potential dramatically increased (Figure 4). The TCE-mineralization capacity persisted into the final post-test phase for all three groups but at lower levels than observed during the multiple-nutrient injection phase (Figure 4).

Hierarchical clustering based on the percentage of TCE mineralized

When the results from enriched TCE-mineralization were further investigated through HCA, they revealed a well group pattern different from that observed with methane concentrations or with enumerations of methanotrophs (Table 1). Groundwater-monitoring wells clustered into four groups (Table 1) on the basis of the TCE-mineralization data. The average percentage of TCE mineralized for groups T-1,T-2, and T-3 had similar values of 6.7, 8.0, and 8.0, respectively, whereas group T-4 (well MHT-4C) exhibited the highest TCE-degrading potential (16.1%) and was separated as an individual group member. Monitoring wells MHT-2C, 5C, 6C, 9C, and 11C grouped together (group T-1) and were related to group T-2 (SI of 0.35), which

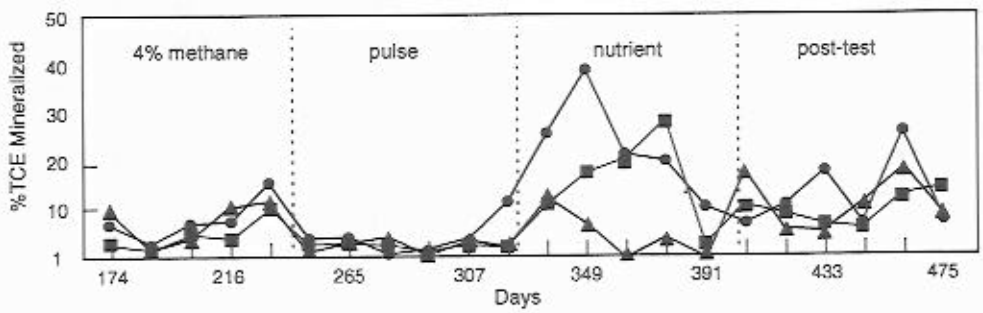

Figure 4 Average percentage of TCE mineralized (under enriched conditions) in groundwater samples collected from each monitoring well during the 4% methane-injection phase through the post-test phase. The monitoring wells were grouped on the basis of the methane concentration hierarchical cluster analysis (group G-1, ■; group G-2, ●; group G-3, ▲). Groups G-3 (near the extraction horizontal well) and G-2 (between both horizontal wells) were considered to be within the zone of effect, whereas group G-1 was adjacent to the zone of effect.

contained monitoring wells MHT-1C and 3C. Well groups T-1 and T-2 were distantly related to group T-4. The remaining monitoring wells (MHT-7C, 8C, 10C, and 9B) clustered in group T-3, which showed no relationship (SI = 0) to the other T-group of wells. PCA on TCE-mineralization data determined that the first four sampling periods (days 335, 349, 363, and 377) in the multiple-nutrient injection phase accounted for the most variance between monitoring well groups; these periods showed the largest observed sample differences in the percentage of TCE mineralized.

Examination of the multiple-nutrient injection phase

An increase in TCE mineralization was exhibited in response to multiple-nutrient injection. PCA showed that the early sampling periods of the multiple-nutrient injection phase were important for stimulating TCE mineralization. Methane concentration, methanotrophic density, percentage of TCE mineralized, and chloride concentration data, recorded as the average for each monitoring well over the multiple-nutrient injection phase, were interpolated and plotted as contour maps (Figures 5–8, respectively).

During multiple-nutrient injection (phase 7), the average methane concentration ranged from 2 to 120 μg L^{-1} in groundwater (Figure 5). The higher concentrations of methane for this phase were located between both horizontal wells and aligned with the injection horizontal well. Monitoring wells in group G-2 (MHT-4C, 6C, and 7C) were within the zone of effect and had groundwater methane concentrations of 40–116 μg L^{-1} (Figure 5). Group G-3 wells (MHT-2C and 11C) considered within the zone of effect, but located outside the extraction horizontal well, showed groundwater methane concentration averages of 5–6 μg L^{-1} for phase 7 (Figure 5). Monitoring wells of group G-1 (MHT-1C, 3C, 8C, and 9C) were more remote and exhibited groundwater methane concentrations of $\leq$5 μg L^{-1}, with the exception of well MHT-10C, which exhibited an average groundwater methane concentration of 20 μg L^{-1} (Figure 5).

Densities of methanotrophs ranged from 1.7 to 5.1 log base 10, which corresponded to 50 to 150 000 cells ml^{-1} (Figure 6). Higher populations of methanotrophs (10^4–10^5 cells ml^{-1}) were located between both horizontal wells and extended along the extraction horizontal well (Figure 6).

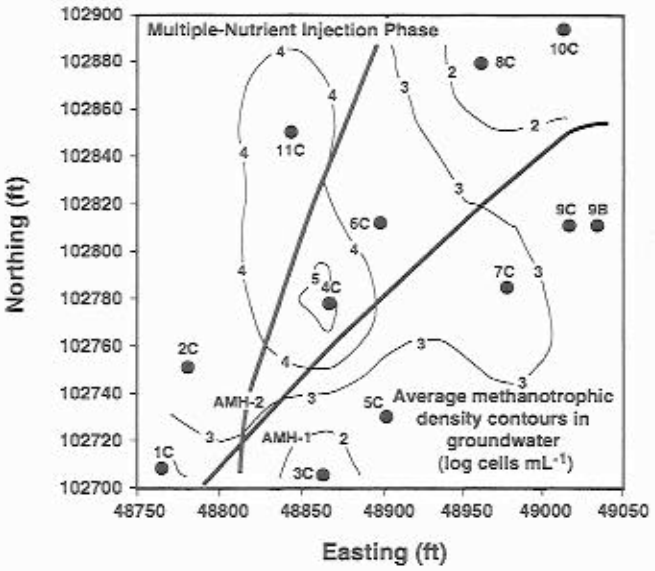

Figure 6 A contour map based on the average methanotrophic densities (log cell ml^{-1}) observed in each groundwater-monitoring well (●) during the multiple-nutrient injection phase. Average densities of methanotrophs ranged from 1.7 to 5.1 log base 10. Higher populations of methanotrophs were found between both horizontal wells and along the extraction horizontal well (AMH-2).

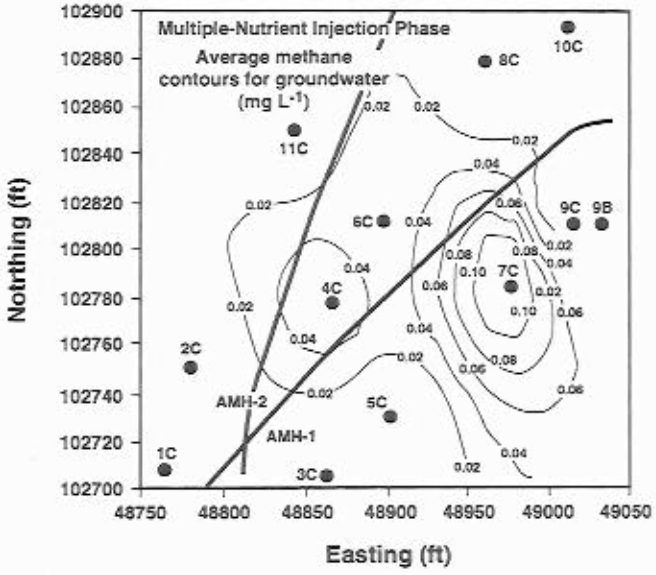

Figure 5 A contour map based on the average methane concentration (μg L^{-1}) observed in each groundwater-monitoring well (●) during the multiple-nutrient injection phase. Methane concentration averages ranged from 2 to 120 μg L^{-1}. The larger concentrations of methane were found between both horizontal wells and aligned with the injection horizontal well (AMH-1).

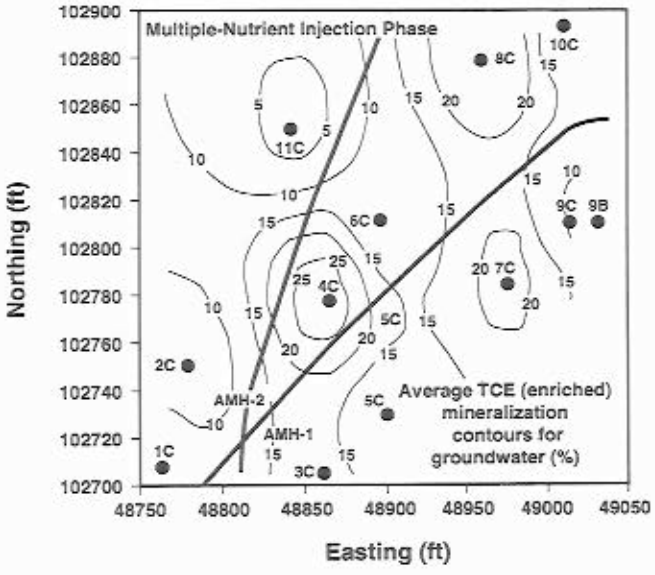

Figure 7 A contour map based on the average percentage of enriched TCE mineralization observed in each groundwater-monitoring well (●) during the multiple-nutrient injection phase. Enriched TCE mineralizations averaged between 4% and 27%. The major area of TCE degradation potential was observed between both horizontal wells and along the injection horizontal well (AMH-1).

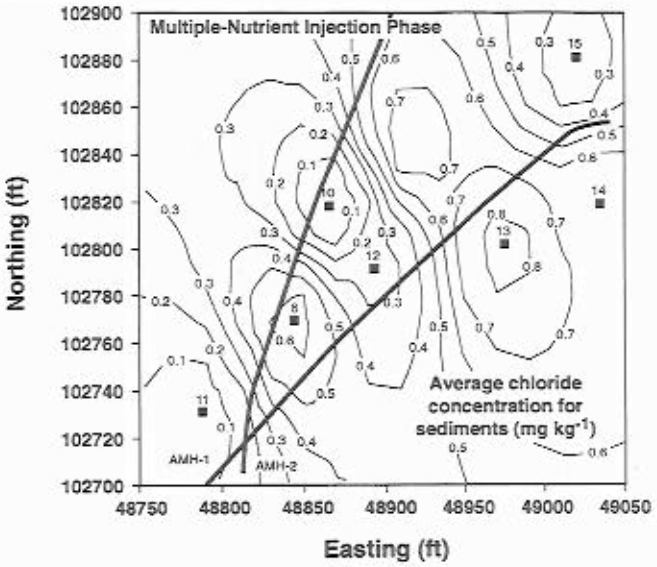

Figure 8 A contour map based on the average increase in chloride concentration (mg kg^{-1}) observed in sediments (■) recovered from coreholes MHC-9 to MHC-15 following the multiple-nutrient injection phase. Prior to methane injection, the chloride concentration in sediments averaged 1.02 ± 0.14 mg kg^{-1}. Chloride concentrations increased in phase 7 sediments (30–40 m depths) and averaged between 0.35 and 1.18 mg kg^{-1}. Increased sediment chloride concentrations were oriented between both horizontal wells and along the injection horizontal well (AMH-1).

Groundwater from monitoring wells within the zone of effect exhibited average densities of methanotrophs ≅1900 cells ml^{-1}, whereas groundwater from areas adjacent to the zone of effect showed average densities of methanotrophs ≅180 cells ml^{-1}.

The major area of TCE biodegradation potential (as shown by the enriched TCE mineralization assays) was between both horizontal wells and along the injection horizontal well (Figure 7). Groundwater from monitoring wells MHT-4C and 6C, within the zone of effect, and well MHT-8C, adjacent to the zone of effect, exhibited high TCE-degradation potentials (>20% TCE mineralized) (Figure 7). Although the groundwater exhibited high TCE-mineralization capacities, these monitoring wells received the two lowest methane doses (Table 1). These results substantiate that methane dosing had little effect on enriched TCE mineralization (Figure 5).

Chloride concentration in sediments

Increased sediment chloride concentration from 1.02 ± 0.14 mg kg^{-1} before methane injection to 1.70 ± 0.41 mg kg^{-1} after the multiple-nutrient injection phase provided direct chemical evidence of TCE degradation. Average increased chloride concentrations for the phase 7 sediments (30–40 m bgs) ranged between 0.35 and 1.18 mg kg^{-1} (Figure 8). The largest increases in chloride concentration were observed between both horizontal wells and aligned with the injection horizontal well (Figure 8). The locations of elevated chloride corresponded to regions of high TCE mineralization as evidenced by: (1) a strong inverse correlation ($r = -0.321$, $P < 0.0001$ [13]) between TCE and chloride concentrations in groundwater (data not shown); and (2) mineralization potential, particularly along the injection horizontal well (Figures 7 and 8), where nitrogen and phosphorus were provided by the multiple-nutrient injection treatment. Additional evidence of increased *in situ* metabolism was significantly ($P < 0.009$) increased groundwater conductivity. For example, well MHT-2C, (within the zone of effect) and well MHT-8C (adjacent to the zone of effect) exhibited average conductivity (and standard error) of 0.051 (± 0.010) and 0.065 (± 0.012), respectively, during the multiple-nutrient injection phase (phase 7) (data not shown). In contrast, average conductivity during phases 4–6, for well MHT-2C ranged from 0.027 to 0.034 (± 0.006) and for well MHT-8C ranged from 0.037 to 0.043 (± 0.005).

Discussion

Changes in populations of methanotrophs and aerobic TCE-degradative capacities during the treatment phases were related to the dosing effects of methane and nutrient additions. After the addition of methane to the subsurface, densities of methanotrophs increased several orders of magnitude from <1 cell ml^{-1} prior to methane injection to $>10^5$ cells ml^{-1} afterward, and densities within well groups increased as methane concentrations increased (Figures 2 and 3). During the 1% methane-injection phase, methanotrophs were first observed in groundwater within the zone of effect [25,26]. Methanotrophs within the zone of effect grew to densities 100 times greater than densities adjacent to the zone of effect (Figure 3). Observed densities of methanotrophs strongly correlated ($r = 0.688$, $P < 0.05$ [13]) with a more conservative method for enumerating methanotrophs, which was based on the measurement of methane consumption performed at SRS [8].

The growth of densities of methanotrophs throughout the demonstration site occurred during the 4% methane-injection phase when methane migrated to remote regions of the site because it had not been consumed within the zone of effect. During the addition of 4% methane, methanotrophs increased from less than 1 cell ml^{-1} to greater than 100 cells ml^{-1} in groundwater from outlying wells (adjacent to zone of effect), but still remained high (10^4 cells ml^{-1}) within the zone of effect [25,26]. To further increase the distribution of microbial biomass and activity, a pulsed-methane-and-air-phase was initiated. The pulsed phase was based on a study at Moffett Field by Semprini *et al* [32], who used a model to estimate how the microbial growth would be distributed throughout the test site by pulses of methane and oxygen. Increased biomass of methanotrophs became dispersed throughout the SRS-integrated demonstration site as evidenced by increases in densities of methanotrophs (background levels of <1 cell ml^{-1}) in groundwater from the remote wells (Figure 6).

Increased densities of methanotrophs during the methane-injection phase were consistent with results from laboratory microcosm, bioreactor, and soil column studies, which showed that the addition of methane increased populations of methanotrophs and TCE degradation [8,9,16,23,28,39]. Field pilot studies by Semprini *et al* [32] exhibited increased methanotrophic activity after amending the subsurface with methane. These researchers found that concentrations of methane decreased while CO_2

concentrations increased; this correspondence was a measure of methanotrophic activity [32]. The SRS *in situ* demonstration used both chemical and microbiological methods to determine methanotrophic activity [13].

A spike in methane concentration was observed in groundwater during multiple-nutrient injection for well group G-2 (Figure 2); the spike coincided with increased methanotrophic densities for that group (Figure 3). The increased methanotrophic densities occurred within the zone of effect, whereas groundwater from wells adjacent to the zone of effect experienced decreased methane concentrations and decreased methanotrophic densities (Figures 2 and 3). Presumably, these decreases were a result of methane consumption and microbial growth within the zone of effect; therefore, less methane reached the areas adjacent to the zone of effect. This theory was supported by results of Travis and Rosenberg [34], who used a history-matching model to simulate the *in situ* demonstration results. Their model indicated little dispersion of nutrients (ie methane, nitrogen, and phosphorus) beyond the injection horizontal well during the multiple-nutrient injection phase.

Doses of other nutrients besides methane may have stimulated TCE degradation. The methane levels in groundwater did not correspond to the TCE-mineralization potential or the sediment chloride concentrations; this lack of correspondence suggested that something in addition to methane stimulated TCE degradation potential (Figures 2, 4, 5, 7, 8). Previous investigations have demonstrated nutrient-limiting conditions (nitrogen and phosphorus) at SRS [4,25,29]. Phelps *et al* [29] demonstrated the greatest stimulation of microbial activity in SRS sediments by additions of water and phosphate; addition of nitrate, sulfate, glucose, or minerals resulted in less stimulation. Palumbo *et al* [25] and Brockman *et al* [4] also investigated the stimulation of bacterial growth and TCE-degradative potentials in SRS groundwater using different nitrogen and phosphorus supplements. The gaseous addition of nitrous oxide and triethyl phosphate to pulsed methane injection facilitated high levels of microbial activity and toxicant degradation throughout the demonstration site (Figures 3 and 4), similar to that demonstrated in laboratory experiments [4,25]. The larger increases in methanotrophic densities were between the horizontal wells and along the extraction horizontal well (Figure 6). The phosphorus addition system developed and used at the SRS integrated demonstration has also been successfully employed to increase petroleum degradation rates at a field site near Traverse City, MI [17], and on Kwajalein Atoll, Republic of The Marshall Islands [38].

As shown by the TCE-mineralization potentials (Figure 7) and chloride concentration data (Figure 8), TCE bioremediation potential during the multiple-nutrient injection was greatest at well groups G-2 and G-3 (within the zone of effect). Furthermore, the inverse correlation between groundwater TCE and chloride, as well as the decreased TCE concentration observed in groundwater and sediments, substantiated the increased TCE mineralization in the zone proximal to the horizontal wells [13]. Well group G-1 degraded half as much TCE as groups G-2 and G-3, but accomplished the degradation more efficiently, using only 10% of the methane and fewer methanotrophs than groups G-2 and G-3 (Figures 5–8). Although the remote regions had an order of magnitude fewer methanotrophs and less available methane and nutrients, they degraded a significant amount of TCE, thus producing chloride. Consequently, the extremities of the demonstration site may have been more efficient at TCE bioremediation with respect to biomass and substrate (more work done per unit resource).

Direct evidence of TCE mineralization was provided by the increased chloride concentration (Figure 8) observed in the sediments. The enhanced TCE-degradation potential observed contributed only circumstantial evidence for the bioremediation of TCE because the mineralizations were based on *in vitro* time-course enrichment studies. Increased chloride concentrations occurred between the horizontal wells and along the horizontal injection well (Figure 8) in locations where both increased methanotrophic densities (Figure 6) and TCE-degradation potentials (Figure 7) occurred. When Travis and Rosenberg [34] used the TRAMP modeling program to estimate TCE removal with and without biodegradation, their simulations indicated a 41% increase in TCE removal by bioremediation in comparison with removal by *in situ* air stripping alone. Furthermore, their model suggested that the addition of nutrients resulted in the bulk of the bioremediation, estimated to be ~780 kg [34]. The effects of nutrient dosing that were observed with enumerations of microorganisms and estimation of degradative potentials, coupled with the chloride concentrations, provided multiple lines of evidence that methane, air, nitrogen, and phosphorus additions were responsible for the success and effectiveness of this integrated *in situ* bioremediation process.

Acknowledgements

We thank the staff at SRS and at the Center for Environmental Biotechnology, The University of Tennessee, Knoxville, TN, who collected and analyzed the groundwater and sediment samples during the demonstration. We are grateful to John Beauchamp and Valerii Fedorov for their statistical analyses. Appreciation goes to Janet Strong-Gunderson and Robert Burlage for editorial comments. This research was supported, in part, by an appointment through the Oak Ridge National Laboratory (ORNL) postdoctoral research associate program administered by the Oak Ridge Institute for Science and Education and ORNL. This demonstration was supported by the Office of Technology and Development within the US Department of Energy's (DOE) Office of Environmental Management, under the Contaminated Plume Containment and Remediation Focus Area. ORNL is managed by Lockheed Martin Energy Research Corp for DOE under contract DE-AC05-96OR22464.

References

1 Alvarez-Cohen L, PL McCarty, E Boulygina, RS Hanson, GA Brusseau and HC Tsien. 1992. Characterization of a methane-utilizing bacterium from a bacterial consortium that rapidly degrades trichloroethylene and chloroform. Appl Environ Microbiol 58: 1886–1893.

2 APHA-AWWA-WPCF. 1989. Argentometric titration of chloride ion. In: Standard Methods for the Examination of Water and Wastewater,

17th edn (Clesceri LS, AE Greenberg and RR Trussell, eds), pp 68–69, APHA-AWWA-WPCF, Washington, DC.
3 Borthen JW, TC Hazen, KH Lombard, BB Looney, SM Pfiffner and TJ Phelps. 1996. Method for phosphate-accelerated bioremediation. US Patent 5 480 549.
4 Brockman FJ, W Payne, DJ Workman, A Soong, S Manley and TC Hazen. 1995. Effect of gaseous nitrogen and phosphorus injection on *in situ* bioremediation of a trichlorothylene-contaminated site. J Hazard Mater 41: 287–298.
5 Corey JC, BB Looney and DS Kaback. 1989. *In situ* remediation system and method for contaminated groundwater. US Patent 5326703.
6 Council on Environmental Quality. 1981. Contamination of groundwater by toxic organic chemicals. US Government Printing Office, Washington, DC.
7 Eddy-Dilek CA, BB Looney, TC Hazen, RL Nichols, CB Fliermans, WH Parker, JM Dougherty, DS Kaback and JL Simmons. 1993. Post-test evaluation of the geology, geochemistry, microbiology, and hydrology of the *in situ* air stripping demonstration site at the Savannah River Site. WSRC-TR-93-369. Westinghouse Savannah River Company, Aiken, SC.
8 Enzien MV, F Picardal, TC Hazen, RG Arnold and CB Fliermans. 1994. Reductive dechlorination of trichloroethylene and tetrachloroethylene under aerobic conditions in a sediment column. Appl Environ Microbiol 60: 2200–2204.
9 Fliermans CB, TJ Phelps, D Ringelberg, AT Mikell and DC White. 1988. Mineralization of trichloroethylene by heterotrophic enrichment cultures. Appl Environ Microbiol 54: 1709–1714.
10 Fogel MM, AR Taddeo and S Fogel. 1986. Biodegradation of chlorinated ethenes by a methane-utilizing mixed culture. Appl Environ Microbiol 51: 720–724.
11 Folsom BR, PJ Chapman and PH Pritchard. 1990. Phenol and trichloroethylene degradation by *Pseudomonas cepacia* G4—kinetics and interactions between substrates. Appl Environ Microbiol 56: 1279–1285.
12 Hazen TC. 1992. Test plant for *in situ* bioremediation demonstration of the Savannah River Integrated Demonstration. WSRC-RD-91-23. Westinghouse Savannah River Co, Aiken, SC.
13 Hazen TC, KH Lombard, BB Looney, MV Enzien, JM Dougherty, CB Fliermans, J Wear and CA Eddy-Dilek. 1994. Summary of *in-situ* bioremediation demonstration (methane biostimulation) via horizontal wells at the Savannah River Site integrated demonstration project. In: *In-Situ* Remediation: Scientific Basis for Current and Future Technologies (Gee GW and NR Wing, eds), pp 137–150, Battelle Press, Richland, WA.
14 Hazen TC and CB Fliermans. 1994. Method of degrading pollutants in soil. US Patent 5 326 703.
15 Henry SM and D Grbic-Galic. 1990. Effect of mineral media on trichloroethylene oxidation by aquifer methanotrophs. Microb Ecol 20: 151–169.
16 Lackey LW, TJ Phelps, V Korde, S Nold, D Ringelberg, PR Bienkowski and DC White. 1994. Feasibility testing for the on-site bioremediation of organic wastes by native microbial consortia. Int Biodeter Biodegrad 33: 41–59.
17 Lawrence AW, DL Miller, JA Miller, RL Weightman, RM Raetz and TD Hayes. 1995. *In situ* bioventing at a natural gas dehydrator site: field demonstration. In: *In-situ* Aeration: Air Sparging, Bioventing, and Related Remediation Processes (Hinchee RE, RN Miller and PC Johnson, eds), pp 581–592, Battelle Press, Richland, WA.
18 Little CD, AV Palumbo, SE Herbes, ME Lidstrom, RL Tyndall and PJ Gilmer. 1988. Trichloroethylene biodegradation by a methane-oxidizing bacterium. Appl Environ Microbiol 54: 951–956.
19 Lombard KH, JW Borthen and TC Hazen. 1994. The design and management of system components for *in situ* methanotrophic bioremediation of chlorinated hydrocarbons at the Savannah River Site. In: Air Sparging for Site Remediation (Hinchee RE, ed), pp 81–96, Lewis Publishers, Ann Arbor, MI.
20 Love T Jr and RG Eilers. 1982. Treatment of drinking water containing trichloroethylene and related industrial solvents. J Am Water Works Assoc 74: 413–425.
21 Malachowsky KJ, TJ Phelps, AB Teboli, DE Minnikin and DC White. 1994. Aerobic mineralization of trichloroethylene, vinyl chloride and aromatic compounds by *Rhodococcus* species. Appl Environ Microbiol 60: 542–548.
22 Nelson DR and JG Zeikus. 1974. Rapid method for the radioisotopic analysis of gaseous end products of anaerobic metabolism. Appl Environ Microbiol 28: 258–261.
23 Niedzielski JJ, RM Schram, TJ Phelps, SE Herbes and DC White. 1989. A total-recycle expanded-bed bioreactor design which allows direct headspace sampling of volatile chlorinated aliphatic compounds. J Microb Meth 10: 215–223.
24 Palumbo AV, JF McCarthy, A Parker, SM Pfiffner, FS Colwell and TJ Phelps. 1994. Potential for microbial growth in arid subsurface sediments. Appl Biochem Biotechnol 45: 823–834.
25 Palumbo AV, SP Scarborough, SM Pfiffner and TJ Phelps. 1995. Influence of nitrogen and phosphorus on the *in situ* bioremediation of trichloroethylene. Appl Biochem Biotechnol 55/56: 635–647.
26 Pfiffner SM, DB Ringelberg, DB Hedrick, TJ Phelps and AV Palumbo. 1995. Subsurface microbial communities and degradative capacities during trichloroethylene bioremediation. In: Bioremediation of Chlorinated Solvents (Hinchee RE, A Leeson and I. Semprini, eds), pp 263–271, Battelle Press, Richland, WA.
27 Phelps TJ, D Ringelberg, D Hedrick, J Davis, CB Fliermans and DC White. 1988. Microbial biomass and activities associated with subsurface environments contaminated with chlorinated hydrocarbons. Geomicrobiol J 6: 157–170.
28 Phelps TJ, JJ Niedzielski, RM Schram, SE Herbes and DC White. 1990. Biodegradation of trichloroethylene in continuous-recycle expanded-bed bioreactors. Appl Environ Microbiol 56: 1702–1709.
29 Phelps TJ, SM Pfiffner, KA Sargent and DC White. 1994. Factors influencing the abundance and metabolic capacities of microorganisms in eastern coastal plain sediments. Microb Ecol 28: 351–364.
30 Riley RG and JM Zachara. 1992. Nature of chemical contaminants on DOE lands and identification of representative contaminated mixtures for basic subsurface science research. DOE/ER-0547T. Office of Energy Research, US Department of Energy, Washington, DC.
31 Semprini L, PV Roberts, GD Hopkins and PL McCarty. 1990. A field-evaluation of *in situ* biodegradation of chlorinated ethenes. Part 2. Results of biostimulation and biotransformation experiments. Ground Water 28: 715–727.
32 Semprini L and PL McCarty. 1991. Comparison between model simulations and field results for *in-situ* biorestoration of chlorinated aliphatics. Part 1. Biostimulation of methanotrophic bacteria. Ground Water 29: 365–374.
33 Shields MS, SO Montgomery, PJ Chapman, SM Cuskey and PH Pritchard. 1989. Novel pathway of toluene catabolism in the trichloroethylene-degrading bacterium *G4*. Appl Environ Microbiol 55: 1624–1629.
34 Travis B and N Rosenberg. 1994. Numerical simulations in support of the *in situ* bioremediation demonstration of Savannah River. LA-12789-MS. Los Alamos National Laboratories, Los Alamos, NM.
35 Tsien HC, GA Brusseau, RS Hanson and LP Wackett. 1989. Biodegradation of trichloroethylene by *Methylosinus trichosporium* OB3B. Appl Environ Microbiol 55: 3155–3161.
36 US Environmental Protection Agency. 1979. Water-related environmental fate of 129 priority pollutants. Report EPA/440/4-79/029a. Office of Water Planning and Standards, Office of Water and Waste Management, US Environmental Protection Agency, Washington, DC.
37 Uchiyama H, T Nakajima, O Yagi and T Nakahara. 1992. Role of heterotrophic bacteria in complete mineralization of trichloroethylene by *Methylocystis* sp strain-M. Appl Environ Microbiol 58: 3067–3071.
38 Walker JF Jr and AB Walker. 1994. Pilot-scale feasibility of petroleum hydrocarbon-contaminated soils *in situ* bioredmediation. In: *In-situ* Aeration: Air Sparging, Bioventing, and Related Remediation Processes (Hinchee RE, RN Miller and PC Johnson, eds), pp 535–541, Battelle Press, Richland, WA.
39 Wilson JT and BH Wilson. 1985. Biotransformation of trichloroethylene in soil. Appl Environ Microbiol 49: 242–243.